FEM ANALYSIS OF JPCP CONCRETE PAVEMENT

Jakub Veselý[*,1], Vít Šmilauer[1]

[*]jakub.vesely.2@fsv.cvut.cz
[1]Czech Technical University in Prague, Faculty of Civil Engineering, Thákurova 7/2077, Prague 6 – Dejvice

Abstract

Pavement analysis and design is an essential part of sustainable and durable road construction. Current analytical methods (Westergaard) may tend to overestimate the effect of different loading scenarios, which can be improved by means of FEM modelling. In this paper, a numerical model for one slab of jointed plain concrete pavement (JPCP) is developed to analyse the pavement subjected to traffic loading.

Keywords

Concrete pavements, JPCP, FEM, traffic loading

1 INTRODUCTION

Concrete pavements are one of the most common solutions for highways or airports due to their high durability when considering mechanical loads. They also have a longer service life compared to bituminous alternatives [1]. Generally, concrete pavements are divided based on the size of the individual slabs and their reinforcement. JPCP (jointed plain concrete pavement) is generally the most commonly used construction type. The individual slabs are typically rectangular, with transverse joints reinforced with dowel bars. The combined effects of traffic loading, together with temperature cycles and drying caused by moisture transport, are the most influential factors affecting the service life of such pavements [2].

The original solutions for concrete pavements originated from Westergard [3]. Analytical solutions were developed mainly until the 1980s, when Huang et al. published their numerical solution specifically for concrete pavements [4]. Further research has focused on solutions for temperature analysis [5], dowel bars [6] and their influence on the stress distribution of neighbouring slabs of concrete pavement [7], or damage to the slab and analysis of cracking and crack propagation [8].

2 METHODOLOGY

For the numerical analysis of concrete pavement (dimensions: 3.75 × 5.0 × 0.29 m), a finite element model in OOFEM software [10] is created. The mechanical model consists of a 3D pavement slab with linear elastic material properties, a 2D subsoil, and interface elements (see Fig.1). The pavement slab is placed on an elastic 2D subsoil plate described using Winkler-Pasternak (W-P) properties. The calibration of the W-P model is shown in [9] and is based on a comparison of deformed shapes resulting from different approaches to subsoil modelling. In this paper, we used the W-P model to reduce the degrees of freedom and computation time while achieving similar results compared to a subsoil modelled as a 3D continuum. It is important to note that the aim of this article is to analyse the concrete pavement, not the subsoil; therefore, the simplification, while using comparable stiffness of the subsoil, is acceptable.

Received 06/02/2025/Accepted 24/04/2025/Published 30/09/2025 DOI 10.13164/juniorstav.2025.25035

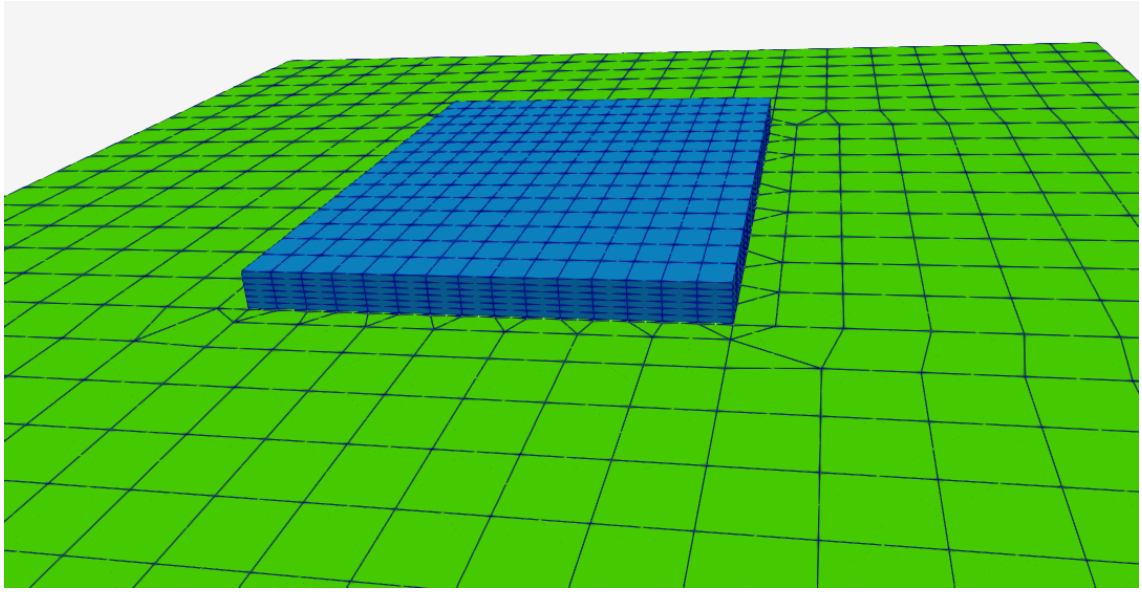

Fig. 1 Mesh for the FEM model of one JPCP slab.

The first classical critical load position according to the literature [5] is at the longitudinal edge of the pavement slab. For slab edge loading, the dimensions play a role: since the slab analysed in this paper has a typical rectangular shape, the stress from the load on the longitudinal edge of the concrete slab should be higher than on the transverse edge.

The subsoil plate with the Winkler-Pasternak model uses material properties c_1 and c_2, representing the normal and shear stiffness of the system [11]. The governing equation is (1):

$$f(z) = c_1 w(z) - c_2 \frac{\partial^2 w(z)}{\partial z^2} \tag{1}$$

where *f(z)* is the surface normal load and *w(z)* is the deflection in the *z*-direction (caused by both traffic loading and the weight of the pavement above). The shear stiffness c_2 mostly influences the deformed shape of the plate.

The interface elements allow separation between the slab and the subsoil, eliminating tensile stress. Both the 3D mesh of the slab and the 2D subsoil mesh have coinciding nodes at the interface. The traction-separation law takes the form of:

$$t_n = k_n \, \delta, \tag{2}$$

$$k_n = k \text{ in compression} \tag{3}$$

$$k_n = 0.01k \text{ in tension} \tag{4}$$

where δ is the displacement between two vertically aligned nodes (one on the bottom surface of the pavement and the second on the top of the W-P plate), with a positive value in separation. k is the compressive stiffness. Shear stiffness is neglected in this simulation. Interface elements can generally lead to convergence issues (see (2), (3), (4)); it is therefore important to find suitable stiffness value for the analysis. The input material properties for the Winkler-Pasternak model, interface elements, and linear elastic properties for concrete are summarized in Tab.1.

Tab. 1 Overview of material properties for FEM analysis in OOFEM.

Material property	Value	Units
E	37.5	GPa
ν	0.2	-
c1	70.0	MNm-3
c2	60.0	MNm-1
k	200	MNm-1

DOI 10.13164/juniorstav.2025.25035

3 RESULTS

The model presented above can be used for any concrete pavement analysis that is loaded with typical traffic loads, while it can also be used for any other mechanical loading scenarios. Within this section, potential critical load positions are analysed: longitudinal edge, transverse edge, corner, and centre of the slab. At the same time, the load is placed within realistic combinations: transverse edge + corner of the slab, longitudinal edge + centre of the slab, and all corners of the slab. To clarify, the load is never placed directly on the edge element of the grid, as this substantially increases the potential error in the calculation due to an inaccurate approximation in the calculation.

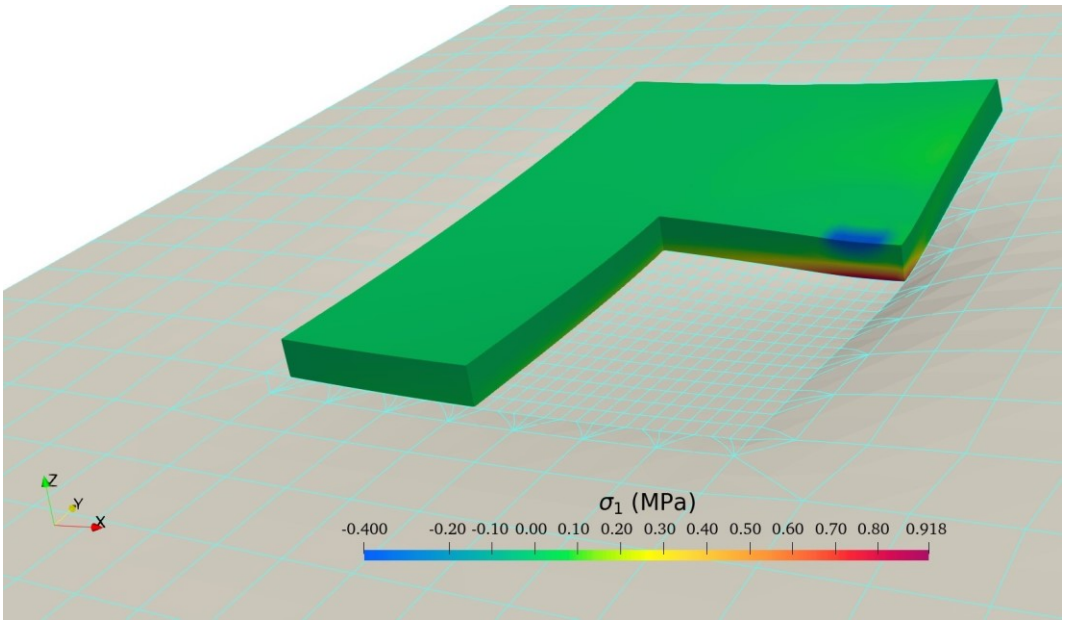

Fig. 2 Stress σ_1 from loading positioned on the longitudinal edge of the JPCP slab.

The maximum value of the tensile stress with the load positioned on the longitudinal edge of the slab is $\sigma_1 = 0.918$ MPa. The tension is located on the bottom surface of the pavement (see Fig. 2).

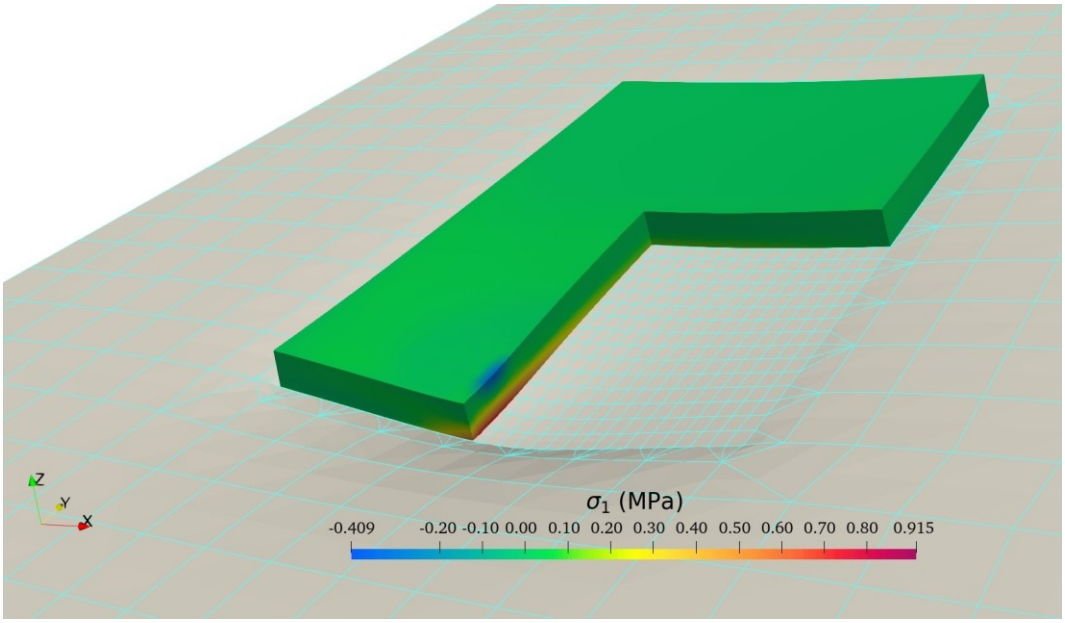

Fig. 3 Stress σ_1 from loading positioned on the transverse edge of the JPCP slab.

DOI 10.13164/juniorstav.2025.25035

When the load is located on the transverse edge of the pavement, the stress is slightly lower than that at the longitudinal edge position. The maximum value of the principal tensile stress in this loading case is $\sigma_1 = 0.915$ MPa. The maximum value is again located at the bottom surface of the slab (see Fig. 3).

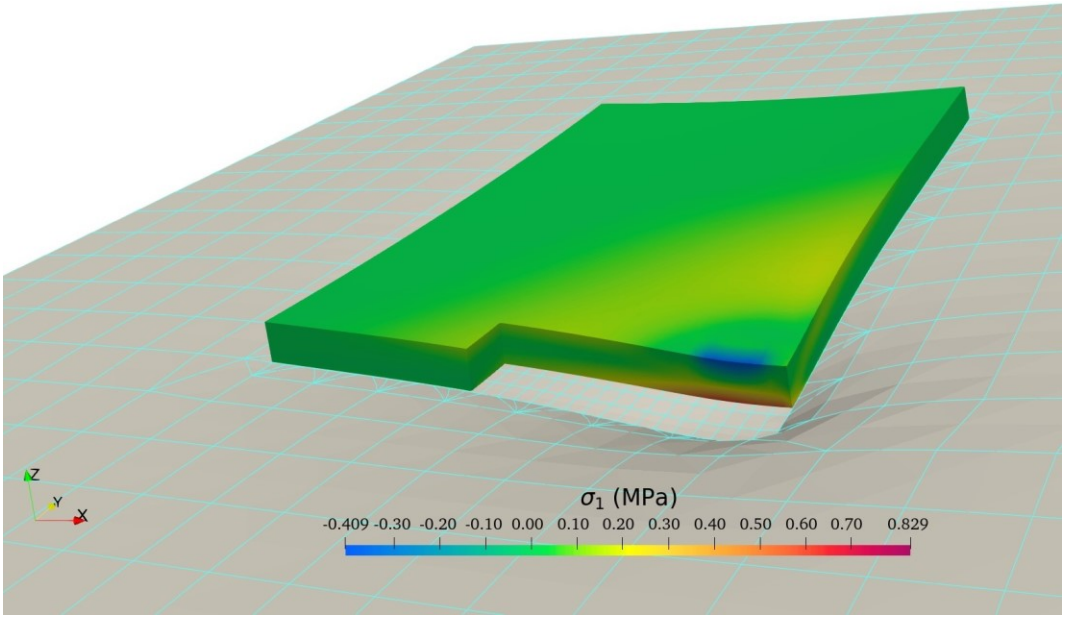

Fig. 4 Stress σ_1 from loading positioned on a single corner of the JPCP slab.

With the load positioned at the corner of the slab, the achieved stress value is lower than at the edge positions, but this position is important due to the potential combination with the transverse edge. It is also important to note that tension is generated on both the top and bottom surfaces of the plate. The maximum value of the main tensile stress is $\sigma_1 = 0.829$ MPa (see Fig. 4). This value is again located at the bottom surface of the slab, but at the same time a tensile stress of approximately $\sigma_1 \approx 0.3$ MPa is generated at the top surface.

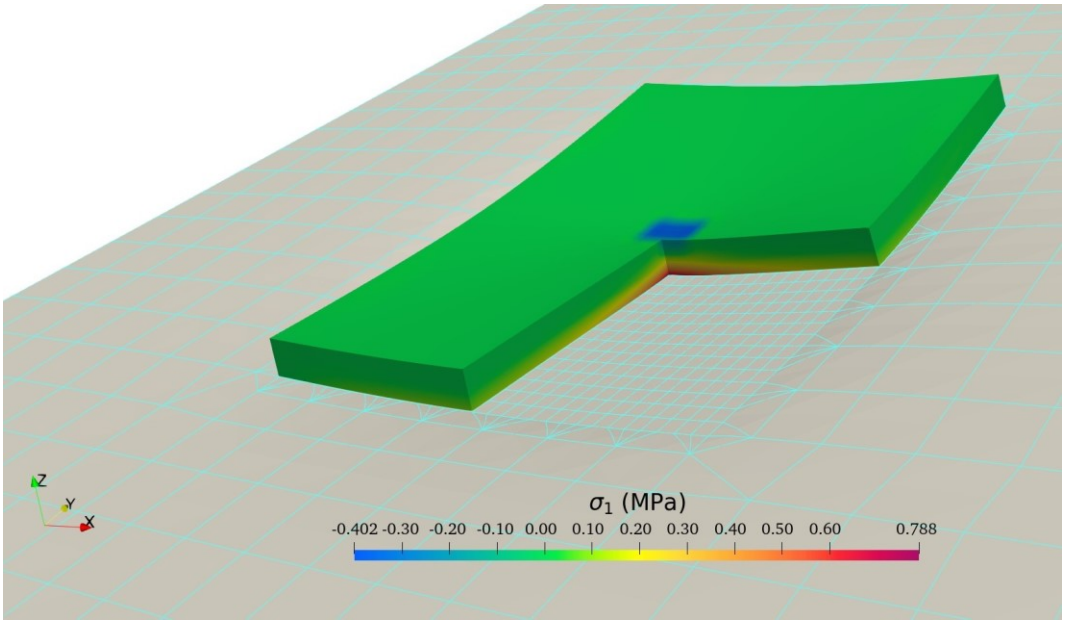

Fig. 5 Stress σ_1 from loading positioned on the centre of the JPCP slab.

The load at the centre of the plate is lower than at the previous positions, but it is again important due to the potential combination with the longitudinal edge of the plate, as they induce a similar deformed shape and this

DOI 10.13164/juniorstav.2025.25035

combination is realistically achievable. The maximum value of the principal tensile stress at the centre of the slab is $\sigma_1 = 0.788$ MPa (see Fig. 5) at the bottom surface.

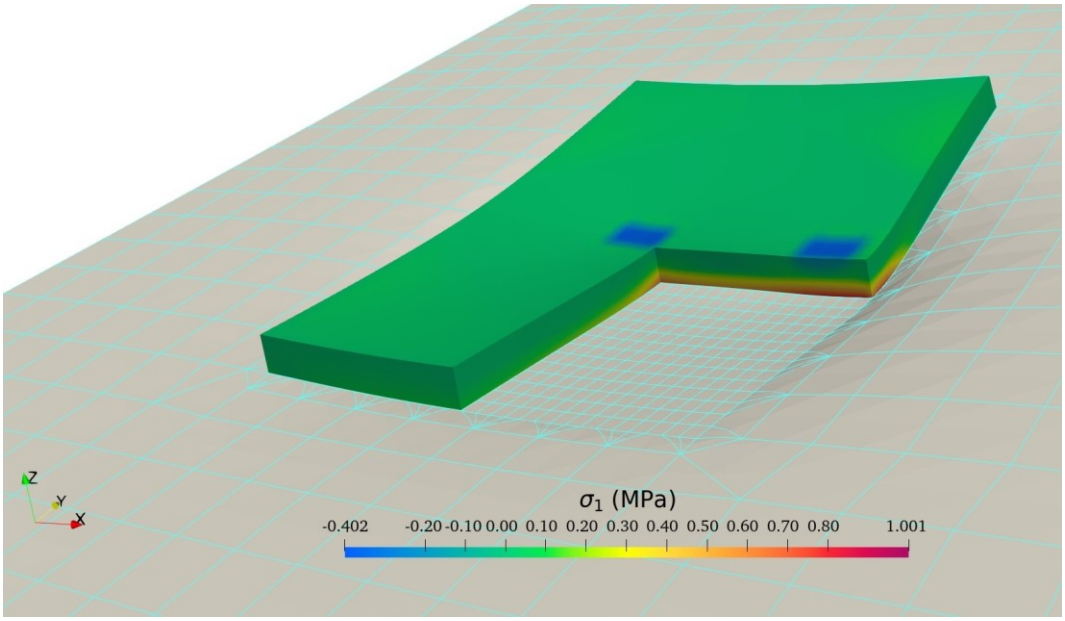

Fig. 6 Stress σ_1 from loading positioned on the longitudinal edge and centre of the JPCP slab.

Therefore, if only one load position is selected at a time, the load position on the longitudinal edge is the decisive load position for this slab dimension. If this position is combined with the load position in the centre of the plate, the stress will increase slightly and the deformed shape will change according to the applied load. The maximum value of the principal tensile stress from this combination of loads (longitudinal edge + centre) is $\sigma_1 = 1.001$ MPa (see Fig. 6). This value is located on the bottom surface of the plate, as when these loads are placed separately.

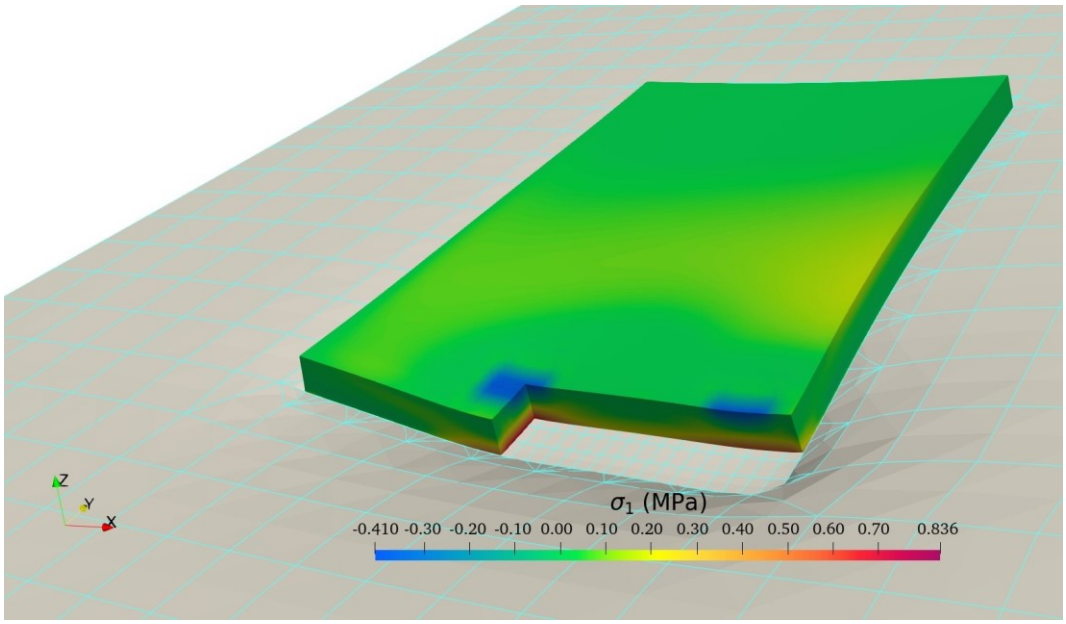

Fig. 7 Stress σ_1 from loading positioned on the transverse edge and corner of the JPCP slab.

If the second critical position on the transverse edge is combined with the position of the load in the corner of the plate, the stress changes; the deformed shape causes a redistribution of stress. The maximum value of the principal tensile stress from this load combination (transverse edge + corner) is $\sigma_1 = 0.836$ MPa (see Fig. 7). This stress value is located on the bottom surface of the plate. At the same time, tensile stress also arises on the top surface of the plate $\sigma_1 \approx 0.3$ MPa.

DOI 10.13164/juniorstav.2025.25035

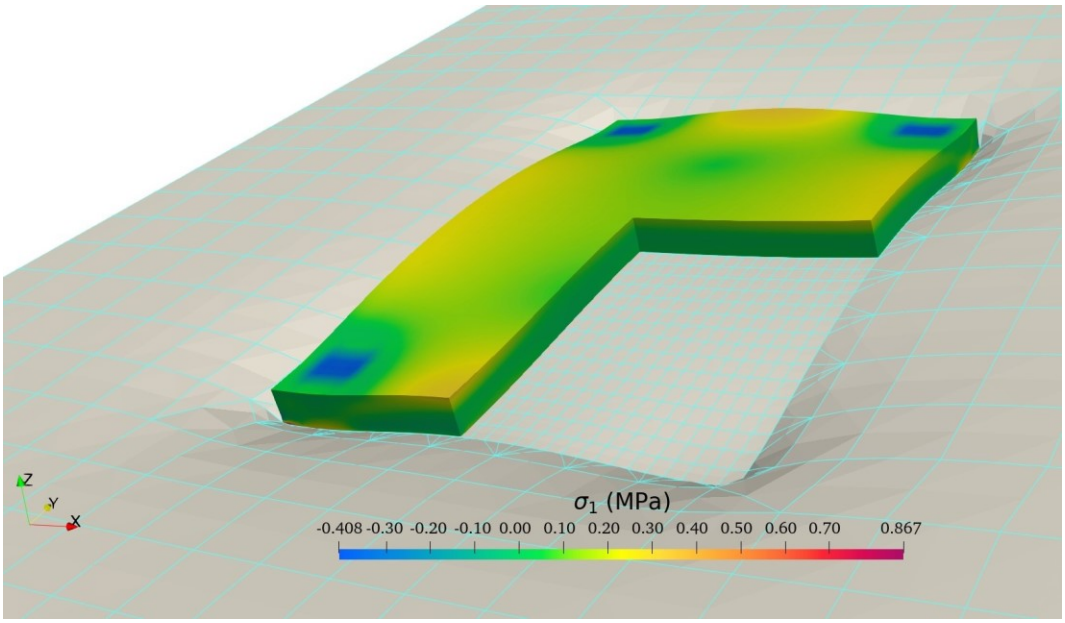

Fig. 8 Stress σ_1 from loading positioned on the corners of the JPCP slab.

If the aim is to induce the highest possible stress on the top surface of the plate, it is advantageous to place the load in all corners of the slab. This configuration will induce a tensile stress of $\sigma_1 = 0.867$ MPa on the bottom surface (see Fig. 8), but also $\sigma_1 \approx 0.53$ MPa on the top surface at the transverse edge of the plate.

4 DISCUSSION

This paper generally aims to improve current methodology for concrete pavement analysis, which is generally constrained by the original assumptions of Westergaard's theory [3]. When comparing the achieved tensile stress from analytical solutions caused by traffic, these tend to be around 2 MPa. According to 3D FEM analysis, these are approximately half (see Tab. 2 and Tab. 3). This is caused primarily by the assumption in the analytical solution that the slab is infinite. This research generally aims to improve pavement design methods by improving the analysis method.

Tab. 2 Overview of resulting tensile stress σ_1 from different loading positions.

Load position	Maximum stress value (σ_1)	Related Fig.
Longitudinal edge	0.918 MPa	2
Transverse edge	0.915 MPa	3
Corner	0.788 MPa	4
Centre	0.829 MPa	5

Tab. 3 Overview of resulting tensile stress σ_1 from different load combinations.

Load combination	Maximum stress value (σ_1)	Related Fig.
Longitudinal edge + centre	1.001 MPa	6
Transverse edge + corner	0.836 MPa	7
All corners	0.867 MPa	8

Results (summarized in Tab. 2 and Tab. 3) show that the maximum tensile stress from a single load is at the longitudinal edge, achieving $\sigma_1 = 0.918$ MPa. When combined with the load positioned in the centre of the slab, the achieved stress is $\sigma_1 = 1.001$ MPa. The highest values of tensile stress are located on the bottom surface of the slab. It is important to acknowledge that for the long-term durability of the pavement, the top surface of the slab is more important (temperature and drying). The highest value on the top surface is achieved when the load is positioned in all four corners ($\sigma_1 = 0.53$ MPa).

DOI 10.13164/juniorstav.2025.25035

5 CONCLUSION

This paper summarizes the effects of traffic loading on a single JPCP concrete pavement slab. The critical loading position confirms the assumption based on the classical analytical solution by Westergaard. The results are summarized as follows:

- Loading at the longitudinal edge is the critical position for JPCP pavements (σ_1 = 0.918 MPa).
- A combination of various positions results in higher stress than a single load (σ_1 = 1.001 MPa).
- The results confirm the assumptions based on classical theories.

Results of this paper will be used in further research focused on developing a method to analyse the fatigue performance of concrete pavements under a combination of temperature, drying, and traffic loading scenarios, in order to improve the design and durability of concrete pavements.

Acknowledgements

We acknowledge financial support for this work from the Czech Science Foundation under project number 25-15501S.

References

[1] LAY, M. G. Handbook of road technology. 4th ed. CRC Press, 2009. ISBN 0-367-86487-8.
[2] GASCH, T., MALM, R., AND ANSELL, A. A coupled hygro-thermo-mechanical model for concrete subjected to variable environmental conditions. International Journal of Solids and Structures [online], 2016, 91, 143–156, https://doi.org/10.1016/j.ijsolstr.2016.03.004
[3] WESTERGAARD, H. M. Stresses in concrete pavements computed by theoretical analysis. Public roads, 1926.
[4] IOANNIDES, A. M. Concrete pavement analysis: the first eighty years. International Journal of Pavement Engineering [online], 2006 7(4), 233–249. Available at: https://doi.org/10.1080/10298430600798481
[5] MACKIEWICZ, P. Thermal stress analysis of jointed plane in concrete pavements. Applied Thermal Engineering [online], 2014, 73(1), 1169–1176. Available at: https://doi.org/10.1016/j.applthermaleng.2014.09.006
[6] SADEGHI, V., HESAMI, S. Investigation of load transfer efficiency in jointed plain concrete pavements (JPCP) using FEM. International Journal of Pavement Research and Technology [online], 2018, 11(3), 245–252. Available at: https://doi.org/10.1016/j.ijprt.2017.10.001
[7] BRONUELA, L., RYU, S., AND CHO, Y. H. Cantilever and pull-out tests and corresponding FEM models of various dowel bars in airport concrete pavement. Construction and Building Materials [online], 2015, 83, 181–188. Available at: https://doi.org/10.1016/j.conbuildmat.2015.02.066
[8] SINGH, K., GHOSH, G. Stress behavior of concrete pavement. Materials Today: Proceedings [online], 2022, 55, 246-249. Available at. https://doi.org/10.1016/j.matpr.2021.06.424
[9] VESELÝ, J., ŠMILAUER, V. Thermo-mechanical model for concrete pavement. Acta Polytechnica CTU Proceedings [online], 2021, 30, 121-125. Available at: https://doi.org/10.14311/APP.2021.30.0121
[10] PATZÁK, B. OOFEM—an object-oriented simulation tool for advanced modeling of materials and structures. Acta Polytechnica [online], 2012, 52(6). Available at: https://doi.org/10.14311/1678
[11] BREEVELD, B. J. S.. Modelling the Interaction between Structure and Soil for Shallow Foundations-A Computational Modelling Approach. Master thesis [online], Delft, 2013 [Accessed 01/02/2025]. Available at: https://resolver.tudelft.nl/uuid:f86d6980-d298-4e42-9fa2-3d6c4c261ad1